Simulation of Methane Reforming Reaction for Syngas Production

Sheeba Jilani[*], Rashid Imran Ahmad Khan[a],

[*,a]Department Of Chemical Engineering, Aligarh Muslim University, India.

Abstract - In this work the simulation study of dry reforming of methane was carried out to produce syngas in three different reactors traditional reactor than subsequently in two different membrane reactors Porous and dense Pd–Ag tubular membranes. The reactors have been compared in terms of: experimental results regarding methane, carbon dioxide conversions, reaction product selectivity and hydrogen recovery. The variation of axial flow rates of all gaseous components with reactor length is calculated. The model equations are solved for all the reactors. The simulated results are analyzed by using same operating conditions of feed, temperature and pressure for FBR, porous MR and dense MR. The model is validated with the experimental studies carried out by [7] on dry reforming reaction using Pd-Ag membrane. The comparison of simulated results with the experimental results has been shown in this study. The conversion of CH_4 in Porous MR is lower than the FBR while the conversion of CO_2 is higher MR reactor in comparison with FBR. The main reason for this was that these membranes can be utilized at high temperatures where chemical reactions occur. The results obtained in terms of conversions are combatable with the experimental results found in the literature.

Keywords: **Membrane reactor; dry reforming; Hydrogen recovery; dense and porous membrane**

I. INTRODUCTION

Syngas (A mixture of hydrogen and carbon monoxides) is a building block in the chemical and petrochemical industries such as for the production of ammonia, methanol, phosgene, acetic acid, oxo-alcohols, and higher hydrocarbons[17]. In some cases, either hydrogen or carbon monoxide is required and this can be acquired from the syngas. For example, the biggest consumer of syngas is for ammonia synthesis, which requires only hydrogen while carbon monoxide is used in the production of paints, plastics, pesticides and insecticides with hydrogen as only a by-product. Thus, the production of synthesis gas from methane and carbon dioxide, also known as carbon dioxide reforming of methane (CORM)/ Dry (CO_2) has received strong interests in the past decades and still is an important topic of the current research.

II. REACTIONS AND KINETICS

Dry reforming of methane involves two main reversible reactions to produce synthesis gas which are as follows[12, 13].

$$CH_4 + CO_2 \xleftrightarrow{r_1} 2CO + 2H_2 \quad (\Delta H_{298} = 247.4\ kJ/mol) \quad (1)$$

$$CO_2 + H_2 \xleftrightarrow{r_2} CO + H_2O \quad (\Delta H_{298} = 41.1\ kJ/\ mol) \quad (2)$$

The reforming of methane with CO_2 is reversible and endothermic in nature [1, 14]. The equation 2 represents reverse water gas shift reaction, which occurs in parallel to dry reforming reaction as a side reaction. This reaction is also reversible and is less endothermic in nature.

However the other two undesired side reactions responsible for carbon formation via methane cracking and Boudouard reaction are as follows[5, 7].

$$CH_4 \rightarrow 2H_2 + C \quad (\Delta H^0_{298K} = 75 kJ/mol) \quad (3)$$

$$2CO \leftrightarrow CO_2 + C \quad (\Delta H^0_{298K} = -173 kJ/mol) \quad (4)$$

Ni/Al_2O_3 catalyst has been used for all the reactors. The dry reforming reactions kinetics was studied thoroughly by [1, 15] for the same catalyst Ni/Al_2O_3 which is given as under:

$$r_1 = k_1 \times K_{CH_4}(P_{CH_4} \times P_{CO_2} - P_{CO_2} \times P^2_{H_2}/K_1)/(1 + K_{CH_4} \times P_{CH_4}) \quad (5)$$

$$r_2 = k_2(P_{CO_2} \times P_{H_2} - P_{CO} \times P_{H_2O}/K_2) \quad (6)$$

 DOI : 10.35291/2454-9150.2020.0609

where: k_1 *and* k_2 are the rate constant for the dry reforming reactions and reverse water gas shift reaction respectively
K_{CH4} is the adsorption equilibrium constant of methane
P_i is the partial pressure (for the components)
K_1 *and* K_2 are chemical equilibrium constants for dry reforming reaction and reverse water gas shift reaction which are defied as:

$$k_1 = 7.13\times10^5 \exp[((-10.7\pm1.1)\times10^4 / RT)] mol\, g^{-1}\, bar^{-1} h^{-1}$$

$$k_2 = 15.92 \exp[((-64.8\pm38.0)\times10^3 / RT)] mol\, g^{-1}\, bar^{-2} h^{-1}$$

$$K_{CH_4} = 4.01\times10^{-4} \exp[((74.6\pm26.0)\times10^3 / RT)] bar^{-1}$$

$$P_i = \frac{F_i}{\sum F_i} P_t$$

Chemical equilibrium constants for dry reforming reaction and RWGS reaction have been derived by using thermodynamic properties . The final expressions are as follows:

$$\ln K_1 = -6.091 \ln T - 4.084\times10^{-3} T + 3.0665\times10^{-7} T^2 + \frac{28623}{T} + \frac{63050}{T^2} + 75.624$$

$$\ln K_2 = 1.86 \ln T + 2.70\times10^{-4} T - \frac{5252.30}{T} + \frac{0.582\times10^5}{T^2} - 7.1977$$

on the basis of stoichiometry of dry reforming and RWGS reactions, the rates of consumption/ formation of reaction species are given below[11].

The net rate of consumption of CH_4, $r_{CH_4} = r_1$ (7)

The net rate of consumption of CO_2, $r_{CO_2} = r_1 + r_2$ (8)

The net rate of production of CO, $r_{CO} = 2r_1 + r_2$ (9)

The net rate of production of H_2, $r_{H_2} = 2r_1 - r_2$ (10)

The net rate of production of H_2O, $r_{H_2O} = r_2$ (11)

III. MODEL USED

A schematic of the membrane reactor is shown in Figure 1 [17]. In the dry reforming of methane process, methane and carbon dioxide are continuously fed into the catalytic zone and sweep gas nitrogen is introduced on the permeation zone to carry away the permeated hydrogen [16]. Here methane dry reforming is carried out first in a fixed bed reactor (Traditional) and subsequently it is carried out in porous & dense Pd-Ag membrane tubular reactor [2, 4, 8]. The catalytic membrane reactor is a cylindrical reactor equipped with a membrane. This membrane is inert with respect to chemical reaction and tubular in shape. The tubular membrane divides the reactor in two zones. First zone is shell side zone which is a reaction zone packed with catalyst particles. The reaction occurs in this zone. Second is tube side zone, also called permeate zone where the sweep gas is introduced co-currently with respect to feed to carry away the permeated gases from the permeate zone. The feed contains mainly CH4, CO2 and nitrogen (as diluent) and is fed to the shell side of reactor. The chemically inert sweep gas nitrogen is introduced into the tube side of reactor. Therefore, in the permeate side (tube side) of the reactor, no chemical reaction occurs.

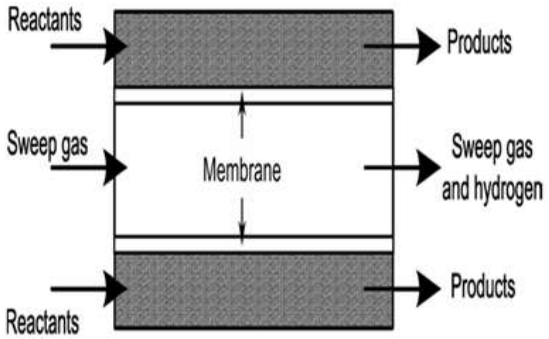

Fig.1 Schematic representation of the membrane reactor

The model used for membrane reactor is based on the certain assumptions which are as follows [10]:

1. Steady state operations as all the state variables are constant.
2. Plug flow behavior has been considered for permeate and reaction zone.

 DOI : 10.35291/2454-9150.2020.0609

3. Isothermal operation
4. Isobaric conditions
5. Inexistence of boundary layer on the membrane
6. Hydrogen diffusion in the membrane is the rate determining step for hydrogen permeation.

The model equations used in this work have been described as under

IV. THE MASS BALANCE EQUATIONS FOR BOTH OF THE REACTORS CAN BE WRITTEN AS:

(a) Fixed bed reactor material balance equation [11].

The general material balance for the i[th] component is defined as:

$$\frac{dF_i}{dz} + W((r_i)(area)) = 0 \quad (12)$$

The above equations for each component can be written as namely for CH_4, CO_2, CO, H_2, H_2O and N_2

$$\frac{dF_{CH_4}}{dz} + W(\pi(r_{CH_4})(R_2^2 - R_1^2)) = 0 \quad (13)$$

$$\frac{dF_{CO_2}}{dz} + W(\pi(r_{CO_2})(R_2^2 - R_1^2)) = 0 \quad (14)$$

$$\frac{dF_{CO}}{dz} + W(\pi(r_{CO})(R_2^2 - R_1^2)) = 0 \quad (15)$$

$$\frac{dF_{H_2}}{dz} + W(\pi(r_{H_2})(R_2^2 - R_1^2)) = 0 \quad (16)$$

$$\frac{dF_{H_2O}}{dz} + W(\pi(r_{H_2O})(R_2^2 - R_1^2)) = 0 \quad (17)$$

$$\frac{dF_{N_2}}{dz} + W(\pi(r_{N_2})(R_2^2 - R_1^2)) = 0 \quad (18)$$

(b) Porous Pd-Ag membrane tubular reactor material balance equation [11]

For Shell side

The general material balance for the i[th] component is defined as:

$$\frac{dF_i}{dz} + W((r_i)(area) - J_i(2\pi R_1)) = 0 \quad (19)$$

The above equations for each component can be written as namely for CH_4, CO_2, CO, H_2, & H_2O

$$\frac{dF_{CH_4}}{dz} + W(\pi(r_{CH_4})(R_2^2 - R_1^2) + J_{CH_4}(2\pi R_1)) = 0 \quad (20)$$

$$\frac{dF_{CO_2}}{dz} + W(\pi(r_{CO_2})(R_2^2 - R_1^2) + J_{CO_2}(2\pi R_1)) = 0 \quad (21)$$

$$\frac{dF_{CO}}{dz} + W(\pi(r_{CO})(R_2^2 - R_1^2) + J_{CO}(2\pi R_1)) = 0 \quad (22)$$

$$\frac{dF_{H_2}}{dz} + W(\pi(r_{H_2})(R_2^2 - R_1^2) + J_{H_2}(2\pi R_1)) = 0 \quad (23)$$

$$\frac{dF_{H_2O}}{dz} + W(\pi(r_{H_2O})(R_2^2 - R_1^2) + J_{H_2O}(2\pi R_1)) = 0 \quad (24)$$

$$\frac{dF_{N_2}}{dz} + W(\pi(r_{N_2})(R_2^2 - R_1^2) + J_{N_2}(2\pi R_1)) = 0 \quad (25)$$

For Tube side

Tube side is permeating side of reactor so there is no chemical reaction. As a result, the material balance equations contain only permeation term and no reaction term, however there is no sweep gas used in Porous MR. The material balance equation for the i[th] component can be written as

$$\frac{dF_i}{dz} = J_i(2\pi R_1) \quad (26)$$

The membrane is porous, therefore all component present in the reaction side get permeated to tube side. The equations for all the components are as follows.

$$\frac{dF_{CH_4}}{dz} - (J_{CH_4}(2\pi R_1)) = 0 \quad (27)$$

 DOI : 10.35291/2454-9150.2020.0609

$$\frac{dF_{CO_2}}{dz} - (J_{CO_2}(2\pi R_1)) = 0 \quad (28)$$

$$\frac{dF_{H_2}}{dz} - (J_{H_2}(2\pi R_1)) = 0 \quad (29)$$

$$\frac{dF_{CO}}{dz} - (J_{CO}(2\pi R_1)) = 0 \quad (30)$$

$$\frac{dF_{H_2O}}{dz} - (J_{H_2O}(2\pi R_1)) = 0 \quad (31)$$

$$\frac{dF_{N_2}}{dz} - (J_{N_2}(2\pi R_1)) = 0 \quad (32)$$

The effect of temperature and mass of gaseous components on the permeability has been found to be very close to that expected from Knudsen diffusion equation. Since the Knudsen diffusivity is inversely proportional to the molecular weight of the gaseous component, the lighter gaseous components diffuse through the membrane faster than the heavier one. The diffusion mechanism through mesoporous membrane can be presented as [15]

$$J_i = \frac{2r\xi}{3\zeta RTd}\sqrt{\frac{8000RT}{\pi M_i}}(P_i - P_i') \quad (33)$$

where Mi is the molecular weight of each component whereas Pi & Pi' is the partial pressure on shell side and tube side respectively.

(c) Dense Pd-Ag membrane tubular reactor material balance equation [11]

For Shell side

The general material balance for the i[th] component is defined as:

$$\frac{dF_i}{dz} + W((r_i)(area) - J_i(2\pi R_1)) = 0 \quad (34)$$

The above equations for each component can be written as namely for CH_4, CO_2, CO, H_2, H_2O& N_2

$$\frac{dF_{CH_4}}{dz} + W(\pi(r_{CH_4})(R_2^2 - R_1^2)) = 0 \quad (35)$$

$$\frac{dF_{CO_2}}{dz} + W(\pi(r_{CO_2})(R_2^2 - R_1^2)) = 0 \quad (36)$$

$$\frac{dF_{CO}}{dz} + W(\pi(r_{CO})(R_2^2 - R_1^2)) = 0 \quad (37)$$

$$\frac{dF_{H_2}}{dz} + W(\pi(r_{H_2})(R_2^2 - R_1^2) + J_{H_2}(2\pi R_1)) = 0 \quad (38)$$

$$\frac{dF_{H_2O}}{dz} + W(\pi(r_{H_2O})(R_2^2 - R_1^2)) = 0 \quad (39)$$

$$\frac{dF_{N_2}}{dz} + W(\pi(r_{N_2})(R_2^2 - R_1^2)) = 0 \quad (40)$$

For Tube side

Tube side is permeating side of reactor so there is no chemical reaction. As a result, the material balance equations contain only permeation term and no reaction term. The sweep gas used in dense MR is N_2.

The membrane is dense, therefore only pure hydrogen get permeated to tube side. The equation can be written as.

$$\frac{dF_{H_2}}{dz} - (J_{H_2}(2\pi R_1)) = 0 \quad (41)$$

$$\frac{dF_{N_2}}{dz} = 0 \quad (42)$$

Where J_{H2} is given by:

$$J_{H_2} = P_{H_2}^o e^{\frac{-E_a}{RT}}((p_{H_2})^{0.5} - (p_{H_2p})^{0.5}) \quad (43)$$

The following definitions have been used for describing the performance of FBR, porous MR and dense MR [6, 7]:

CH_4 conversion (%) = $= \frac{CH_{4,\,feed} - CH_{4,\,out}}{CH_{4,\,feed}} \times 100$ (44)

CO_2 conversion (%) = $\frac{CO_{2,\,feed} - CO_{2,\,out}}{CO_{2,\,feed}} \times 100$ (45)

 DOI : 10.35291/2454-9150.2020.0609

$$H_2 \text{ selectivity } (\%) = \frac{H_{2,out}}{H_{2,out} + CO_{out} + CH_{4,out} + CO_{2,out}} \times 100 \quad (46)$$

$$CO \text{ selectivity } (\%) = \frac{CO_{,out}}{H_{2,out} + CO_{out} + CH_{4,out} + CO_{2,out}} \times 100 \quad (47)$$

V. OPERATING CONDITIONS

This theoretical work deals with the analysis of dry reforming reactions in three different reactors. The mathematical model used for porous MRs consists of a set of twelve differential equations as all the gases permeate through the membrane whereas for dense MR model has eight ODEs as only 2 components permeate through the dense membrane. For FB only six ODEs is used as no membrane is used [11].

Parameter	Value	Parameter	Value
L	0.15 m	d	50 µm
W	4 gm	ϵ	0.6
R	8.314 J/mol-K	F_{CH4}	45 µmol/s
P_t	1 atm	F_{CO2}	45 µmol/s
P_t'	1 atm	F_{N2}	10 µmol/s
τ	3	F_{N2}'	05 µmol/s
R_1'	0.005 m	F_{CH4}'	0.0 µmol/s
R_1	0.00495 m	F_{CO2}'	0.0 µmol/s
R	4 nm	F_{H2}	45×10^{-10} µmol/s

Table 1: Operating and boundary conditions

Here model equations are solved for all the three reactors. The variation of axial flow rates for all the gaseous components with reactor length is calculated at different temperature by keeping the other variables as constants.

VI. RESULTS AND DISCUSSIONS

Simulation results

The simulated results are analyzed by using same operating conditions of feed, temperature and pressure for FBR, porous MR and dense MR. The model is validated with the experimental studies carried out by [7] on dry reforming reaction using Pd-Ag membrane. The comparison of simulated results with the experimental results has been shown in table 1, 2 & 3 for the above different reactors used in this study. It is observed from the tables 1, 2 & 3 the conversion of CH_4 in porous MR is lower than the FBR while the conversion of CO_2 is higher in MRs than the FBR. In this study it is important to mention that the methane reforming temperature range is taken from 623 to 723K because of the reason that at higher temperature carbon deposition takes place on the surface of the catalyst. The experimental average values of CH_4 and CO_2 conversion, and H_2 and CO selectivity, are compared with our simulated results of the FBR, porous MR and dense MR in table 1 table 2 and table 3, for different temperatures. All table reports a direct comparison between the MRs and the FBR in terms of CH_4 and CO_2 conversion.

Considering the temperature range investigated and comparing the tables, show that CH_4 conversion is lower for the MR than the FBR; for example, at 723K, CH_4 conversion is 8.4% for the MR and about 17.4 % for the FBR, it can also be seen that the simulated and experimental values for methane conversion are same. Despite this, experimental value for CO_2 conversion at the same temperature is about 21% for the MR versus 14% for the FBR.

Assuming Knudsen-like diffusion also for CH_4, CO, CO_2 and H_2O (*i.e.* for example, ideal separation factor CO/CO_2 of about 1.25), this evidence could be explained considering that, in the MR, the reverse reaction in section 2 equation number (4) is favoured by the selective permeation of CO with respect to CO_2 throughout the porous Pd–Ag membrane. This comparison demonstrates that, by choosing one reactor instead of the other, a different parameter could be maximized: CH_4 conversion by choosing the FBR, CO_2 conversion by choosing the MR. So, in this case, the choice of the reactor type could depend on the goal of reaction system. A similar consideration can be done by comparing the MRs and the FBR in terms of H_2 and CO reaction selectivity (average values). In fact, Table 3 shows that the maximum H_2 selectivity is 10.5% at 723K for the MR, versus about 12.7% for the FBR at the same temperature. Moreover, 19.5% of CO selectivity is achieved in the MR versus 12.4% for the FBR, at the same temperature of 723K. Again, the goal of maximizing CH_4 conversion leads to maximize H_2 production (FBR), while the goal of maximizing CO_2 conversion leads to maximize CO production (porous MR).

 DOI : 10.35291/2454-9150.2020.0609

Tables for Conversion and selectivity of the different components at different temperatures for the different reactors

Reactors	*Conversion of CH_4 %*		*Conversion of CO_2 %*		*Selectivity of H_2 %*		*Selectivity of CO %*	
	Exp. val.	*Sim. val.*	*Exp. val.*	*Sim. val.*	*Exp. Val.*	*Sim. Val.*	*Exp. val.*	*Sim. Val.*
FBR	0.8	0.831	10.66	11.177	2.11	2.125	3.74	3.913
Porous MR	0.1	0.147	6.7	6.97	1.2	1.80	4.7	4.54
Dense MR	-	0.937	-	10.37	-	3.22	-	3.87

Table 2: Validation of model results of FBR, porous MR dense MR at Temp: 623K,

Reactors	*Conversion of CH_4 %*		*Conversion of CO_2 %*		*Selectivity of H_2 %*		*Selectivity of CO %*	
	Exp. val.	*Sim. val.*	*Exp. val.*	*Sim. val.*	*Exp. Val.*	*Sim. Val.*	*Exp. val.*	*Sim. Val.*
FBR	5.6	5.632	14.22	14.097	4.39	4.278	7.38	7.546
Porous MR	0.3	0.321	15.90	17.74	4.2	4.79	8.9	9.45
Dense MR	-	4.486	-	16.22	-	3.95	-	6.97

Table 3: Validation of model results of FBR, porous MR dense MR at Temp: 673K, Pressure:

Reactors	*Conversion of CH_4 %*		*Conversion of CO_2 %*		*Selectivity of H_2 %*		*Selectivity of CO %*	
	Exp. val.	*Sim. val.*	*Exp. val.*	*Sim. val.*	*Exp. Val.*	*Sim. Val.*	*Exp. val.*	*Sim. Val.*
FBR	17.41	17.957	14.02	16.965	12.68	12.157	12.68	12.971
Porous MR	8.4	8.655	20.60	20.03	10.5	10.84	19.5	19.93
Dense MR	-	19.766	-	28.04	-	3.84	-	13.73

Table 4: Validation of model results of FBR, porous MR dense MR at Temp: 723K,

Axial variation of flow rate in Fixed Bed Reactor (FBR):

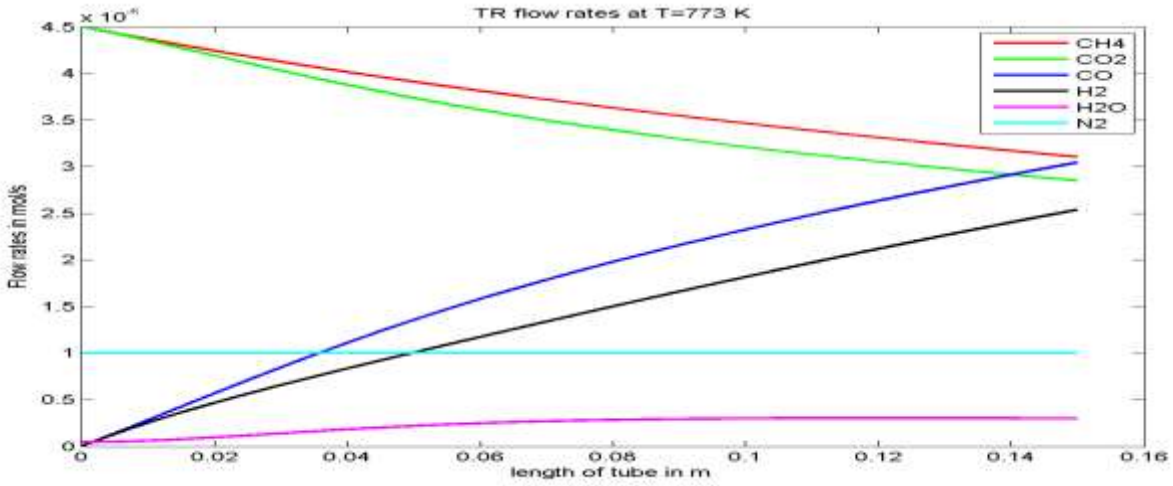

Fig**. 2 Axial variation of flow rate of components in FBR at Temperature 773K**

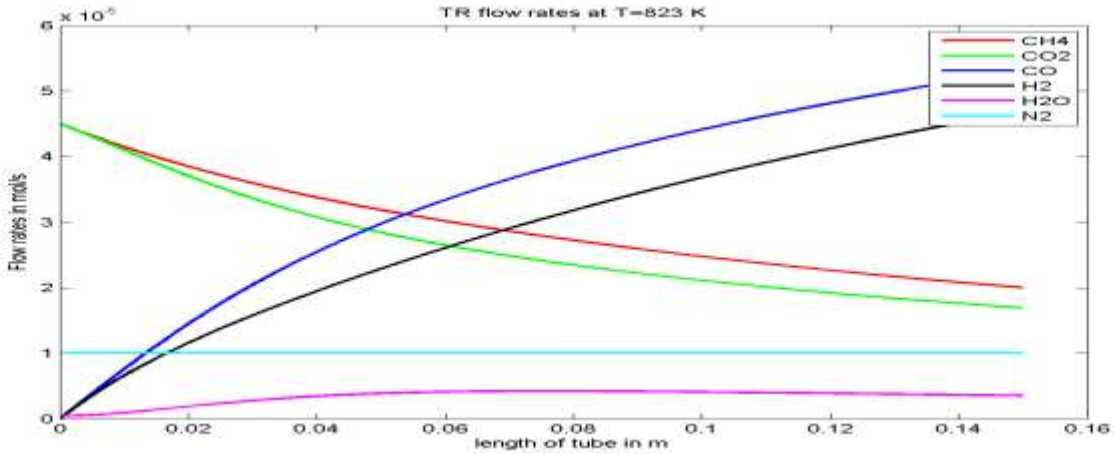

Fig 3 Axial variation of flow rate of components in FBR at Temperature 823K

 DOI : 10.35291/2454-9150.2020.0609

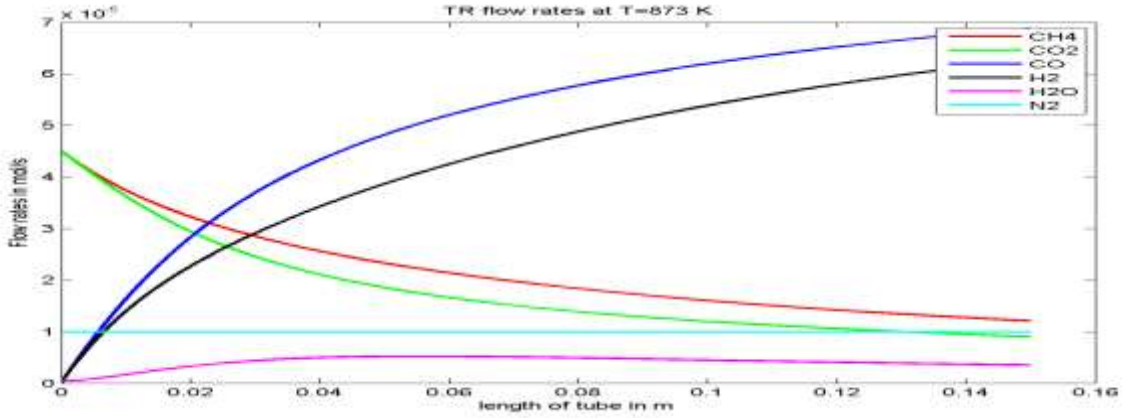

Fig. 4: Axial variation of flow rate of components in FBR at Temperature 873K

Here in the figures 2, 3 & 4 variation of flow rates is shown with the length of the reactor. The temperature range considered for the graph ranges from 773-873K as the kinetics used for the catalyst ranges in between the same temperature range. The flow rate profiles of different gaseous components in the FBR at different temperature are shown in the figures As can be seen from the graph the flow rates of reactants i.e. CH_4 and CO_2 decreases gradually and continuously with the length of the reactor until the equilibrium is reached. The flow rate of CO_2 is lower than CH_4; it is because of the consumption of CO_2 in dry reforming reaction as well as in reverse water-gas shift reaction (RWGS). While CH_4 is consumed in only dry reforming reaction. As the N_2 gas is working as diluents so its flow rate remains constant throughout the length of reactor which is a usual phenomenon. However the flow rates of the products CO and H_2 increases continuously until the equilibrium is achieved. The flow rates of CO is higher than the H_2 this can be explained as the H_2 gas produced in the process is also consumed in RWGS to yield more CO and H_2O whereas CO is produced in both dry reforming and RWGS reaction. The flow rate of H_2O increases slowly and is very small in quantity because the only source of its production is RWGS reaction which is around 3.5µmol/s.

Axial variation of flow rate in Porous Membrane Reactor:

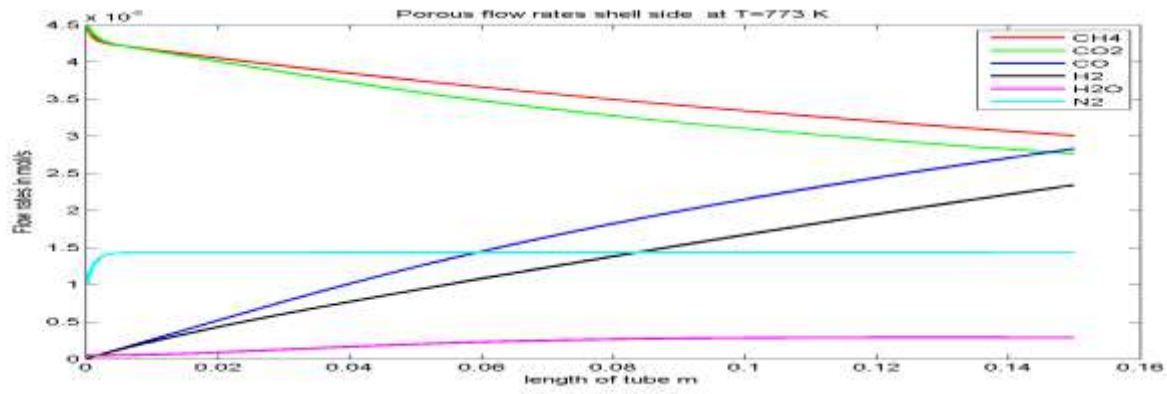

Fig. 5: Axial variation of flow rate of components in Shell side Porous MR at Temp. 773K

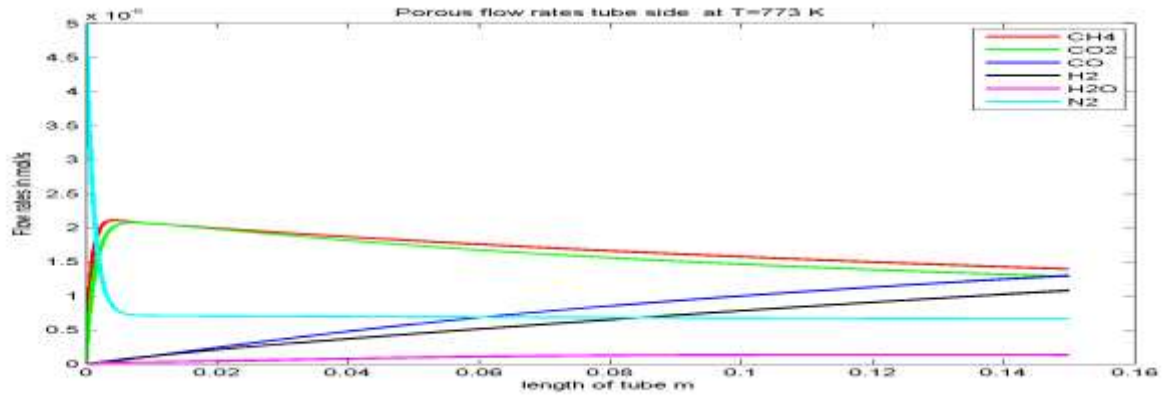

Fig. 6: Axial variation of flow rate of components in Tube side Porous MR at Temp. 773K

 DOI : 10.35291/2454-9150.2020.0609

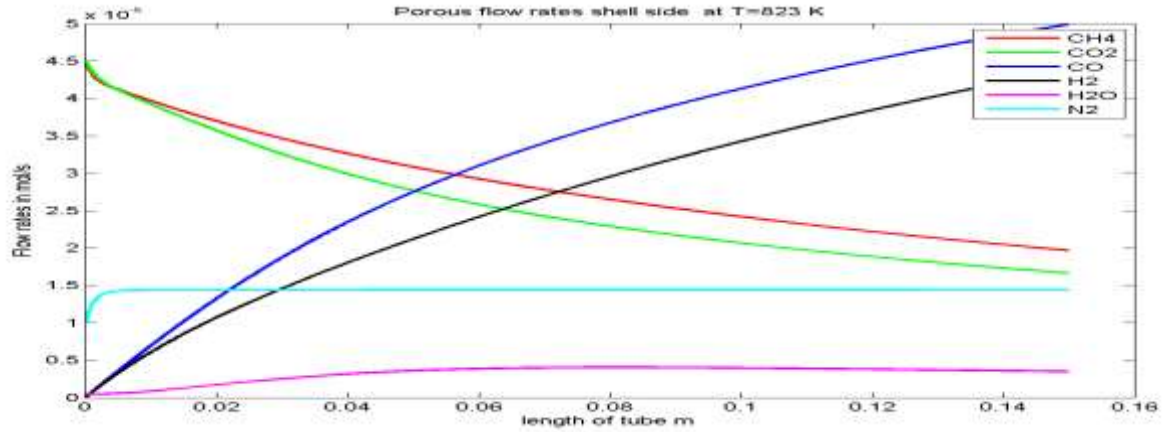

Fig. 7: Axial variation of flow rate of components in shell side porous MR at Temp. 823K

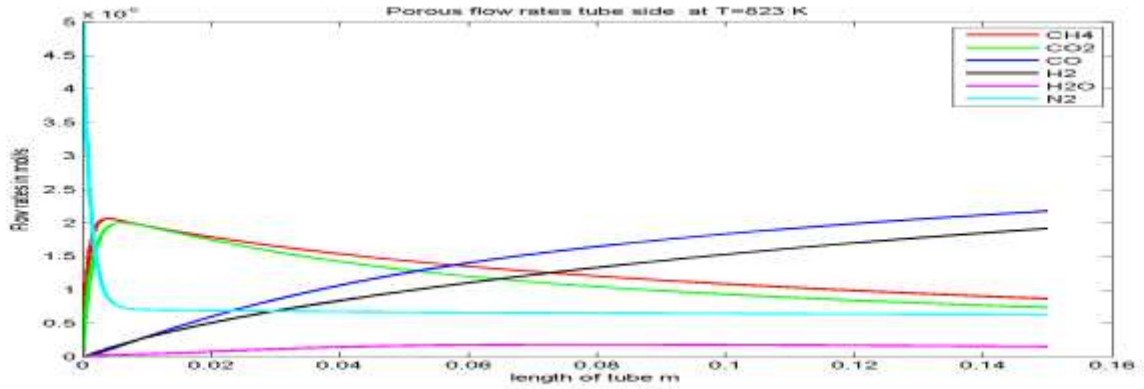

Fig. 8: Axial variation of flow rate of components in tube side porous MR at Temp. 823K

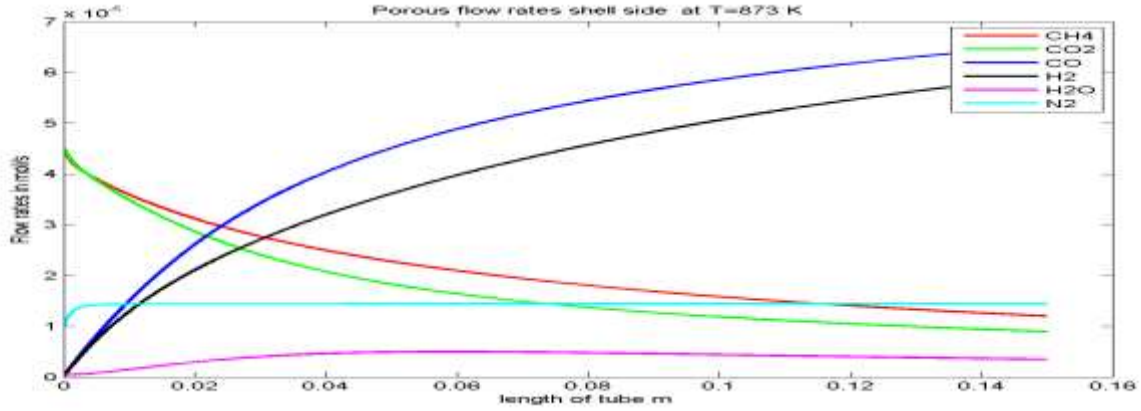

Fig. 9: Axial variation of flow rate of components in Shell side Porous MR at Temp. 873K

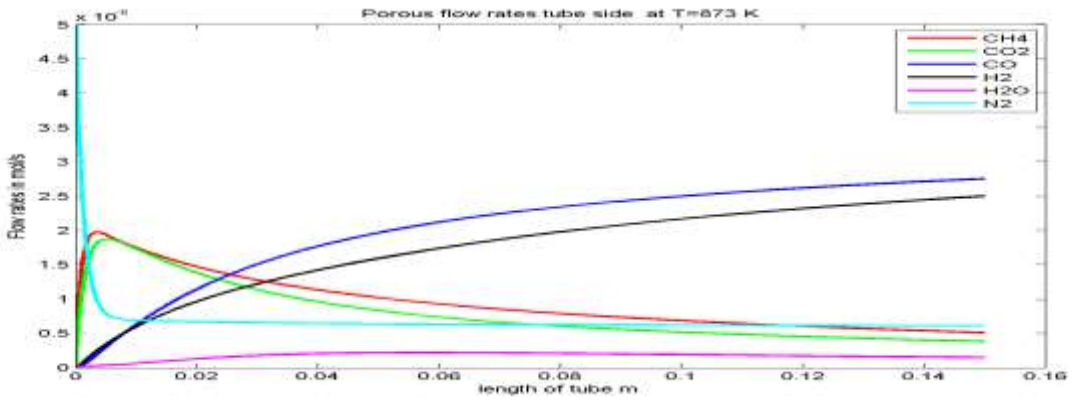

Fig. 10: Axial variation of flow rate of components in Tube side Porous MR at Temp. 873K

For the porous Pd-Ag MR the figures 5, 6, 7, 8, 9 & 10 are shown separately for the reaction (shell) side and the permeate side. Here in this figure porous membrane made of Pd-Ag is used. This porous MR having two sides, shell side and permeate side

 DOI : 10.35291/2454-9150.2020.0609

which is tube side is shown in figure 1. In shell side of the reactor, reaction is taking place here it can be seen that the trends for the flow rates for all the components are similar to that of FBR except for the N_2 whose concentration varies which has been used as sweep gas. The only difference can be seen in the values of the flow rates. In MR the flow rates of reactants CH_4 and CO_2 are lower while the flow rates of product H_2, CO and H_2O are higher than that were obtained in the FBR. This can be justified as the reforming reaction is of reversible character and in this a thermodynamic equilibrium is always present, i.e. equilibrium conversion is thermodynamically limited. This reversibility always limits the maximum conversion of CH_4 in FBR. In this type of reactions the removal of any one or all the products is required to shift the equilibrium to the right, which can be explained by Le Chetelier principle. In dry reforming, the removal of H_2, CO and H_2O from shell side by using membrane in the reactor will shift the equilibrium toward desired direction i.e. product side. Therefore the exit values of the flow rate of component differ from that obtained in FBR. The exit values of the reactants (CH_4 & CO_2) in shell side are recorded as $1.208* 10^{-5}$ & $8.976*10^{-6}$mol/s while in FBR these values of reactants are $1.208* 10^{-5}$mol/s & $9.07*10^{-6}$mol/s respectively. The flow rates of water reported is almost equal in both the reactors which are $3.5*10^{-6}$ & $3.99* 10^{-6}$ with MR is slightly less than the FBR which is obvious due to permeation of water in the tube side. The flow rates of products (H_2 & CO) which are higher in Porous MR because CO produced in two parallel reactions while H_2 is consumed in RWGS reaction. The flow rate of N_2 first increases in the shell side and after reaching to $1.44 * 10^{-5}$mol/s remains constant throughout the process.

Now the tube side which is permeate side of the reactors shown in figure 6. The flow rate of the products (H_2, CO & H_2O) increases along the length of the reactor which only occurs due to the diffusion. This diffusion can be explained by Knudsen Mechanism. This principle suggest that the permeance of component is inversely proportional to the square root of its molecular weight ($1/\sqrt{Mi}$) since molecular weight of H_2 is lower than CO & H_2O so it can permeate at higher rate than CO &H_2O. Also H_2 is consumed in RWGS reaction so its flow rate is smaller than CO. Now the reactants CH_4& CO_2 permeate at higher rate in at the initial length of the reactor but as the reaction goes their rate decreases to a lower value. Beside this N_2 also permeate to this side & their value at the exit comes out to be $6.102*10^{-7}$ mol/s.

Axial variation of flow rate in Dense Membrane Reactor

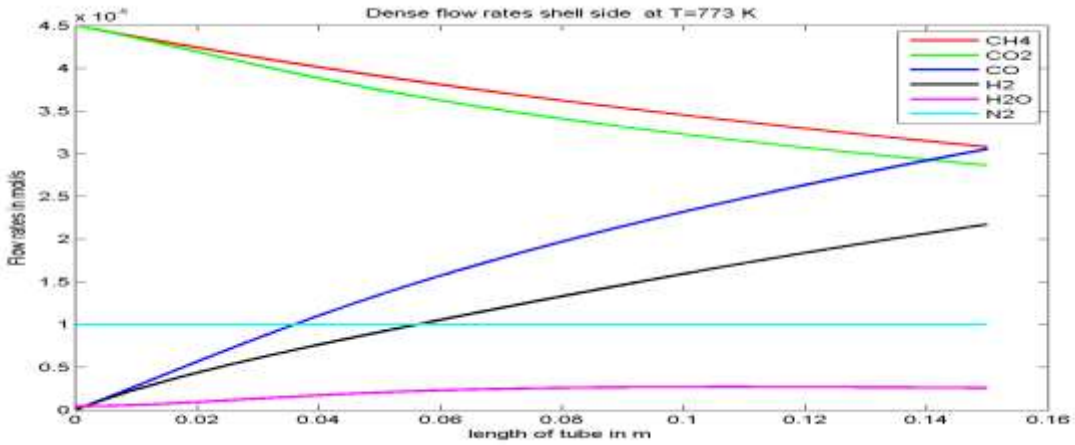

Fig.11: Axial variation of flow rate of components in Shell side Dense MR at Temp. 773K

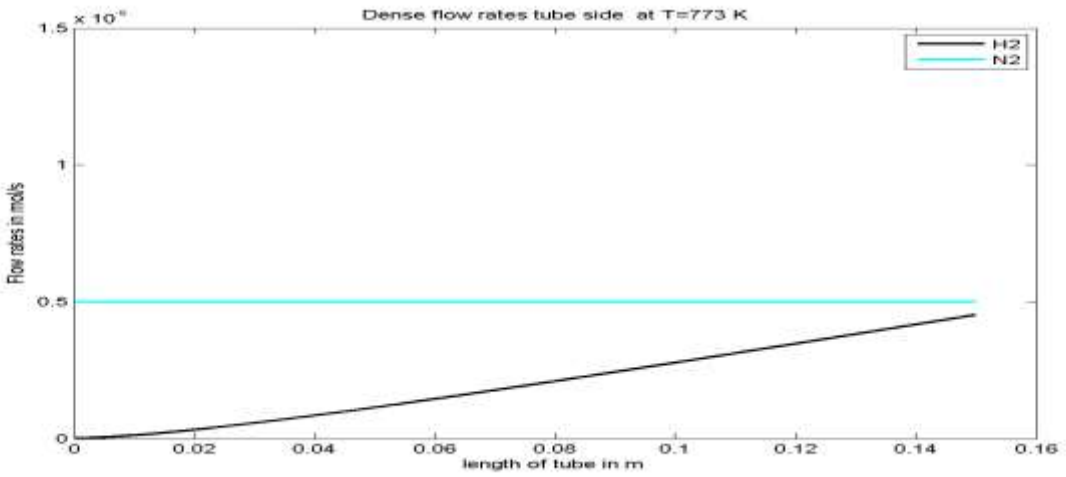

Fig. 12: Axial variation of flow rate of components in Tube side Dense MR at Temp. 773K

 DOI : 10.35291/2454-9150.2020.0609

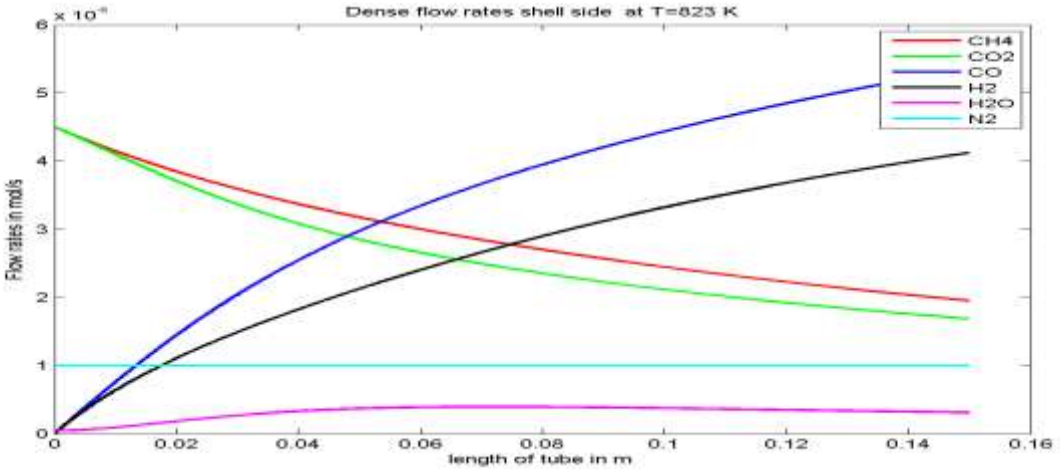

Fig. 13: Axial variation of flow rate of components in Shell side Dense MR at Temp. 823K

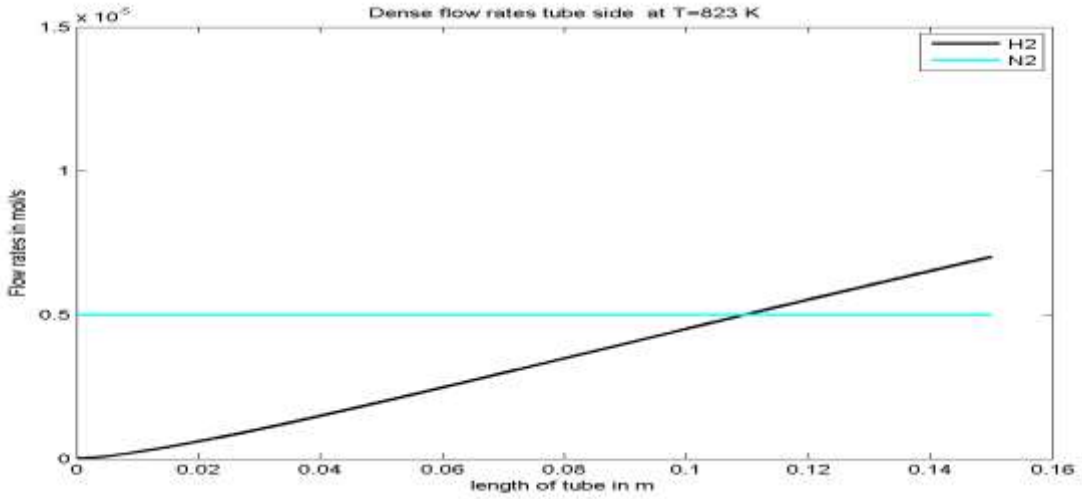

Fig. 14: Axial variation of flow rate of components in Tube side Dense MR at Temp. 823K

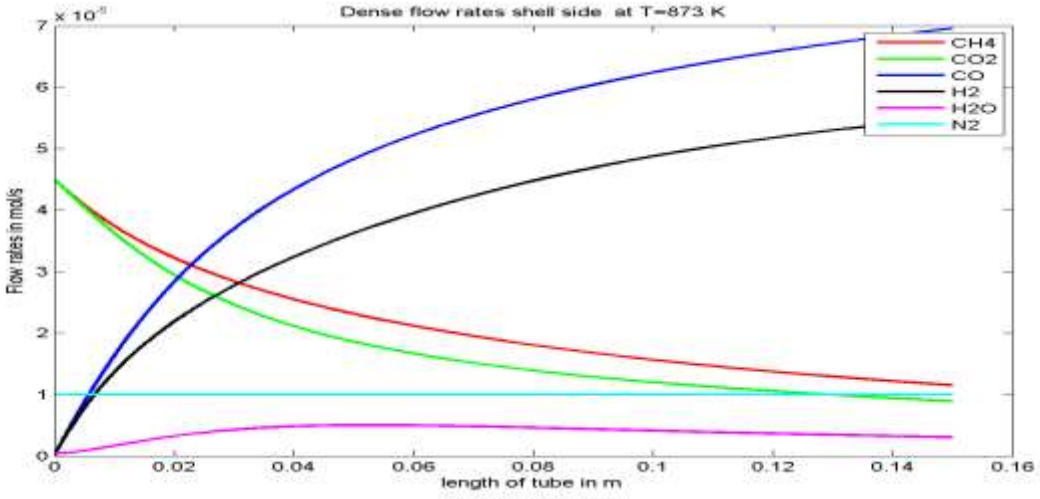

Fig.15: Axial variation of flow rate of components in Shell side Dense MR at Temp. 873K

 DOI : 10.35291/2454-9150.2020.0609

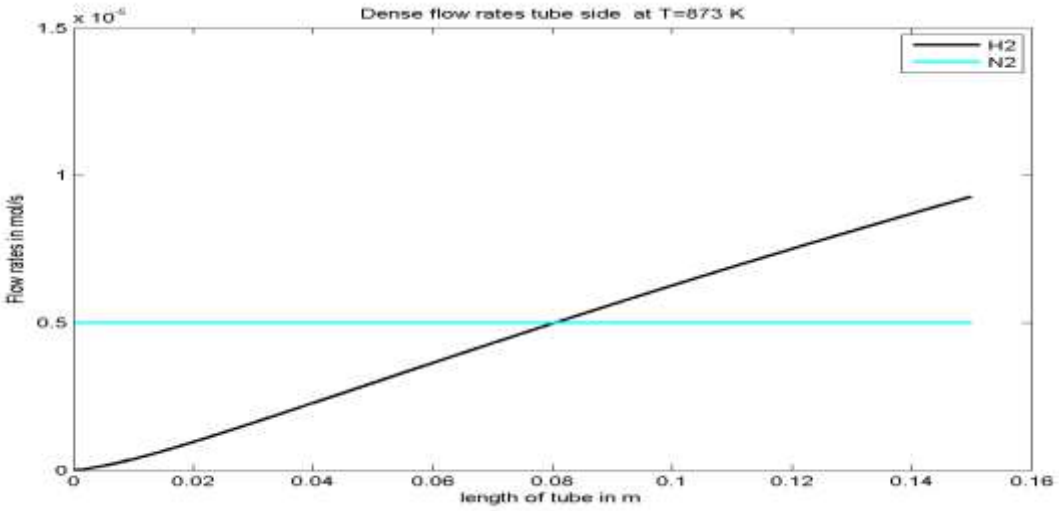

Fig. 16: Axial variation of flow rate of components in Tube side Dense MR at Temp. 873K

Figure 11– 16 shows the flow rates of all the gaseous components in the DMR. A comparison for the flow rates of the reactant and products can be made with FBR and porous MR. As can be seen from the figure 11 the flow rates of the reactants CH_4 & CO_2 are almost same in all types of reactor but the product flow rates in figure 11, 13 and 15 gives a good comparison. For temperature 873K the flow rates of CO & H_2 increases from to FBR to Porous MR to Dense MR. This can be understood as the dense MR allows only H_2 to permeate, which shift the equilibrium & can be explained by Le Chatelier principle. A good amount of H_2 yield can be obtained in the DMR because it is selective for the H_2 & N_2 permeation. The tube side of the DMR shows a good permeation of H_2 in the tube side.

In the case of dry reforming system the reactions that are favoured by the hydrogen permeation are the ones in which the methane is involved. The carbon deposition decreases in the dense membrane reactor with respect to the FBR and porous MR. which is due to Le Chatelier principle; the hydrogen permeating through the dense membrane reduces the carbon deposition in the reaction while it increases the carbon deposition in reaction (4). Evidently the positive effect of the chemical reaction is predominant with negative effect of the reaction (4). The overall effect is the reduction of the carbon deposition in the dense MR. Thus the CH_4 conversion is close to the equilibrium value and the carbon deposition is lower than the one observed in FBR and the porous MR.

Effect of temperature on CH_4 conversion in porous MR & dense MR

Reaction temperature plays an important role in a reactor performance figure 17 & 18 shows that the variation in conversion of CH_4 with the temperature for porous and DMR. Owing to the endothermic nature of reaction, the percentage conversion increases with increase in temperature for both the reactors. However it can be seen from graphs that the DMR has higher methane conversion than the corresponding porous MR under the same conditions which is due to the fact that dense MR is only permselective to H_2 thus leading to higher conversion of methane

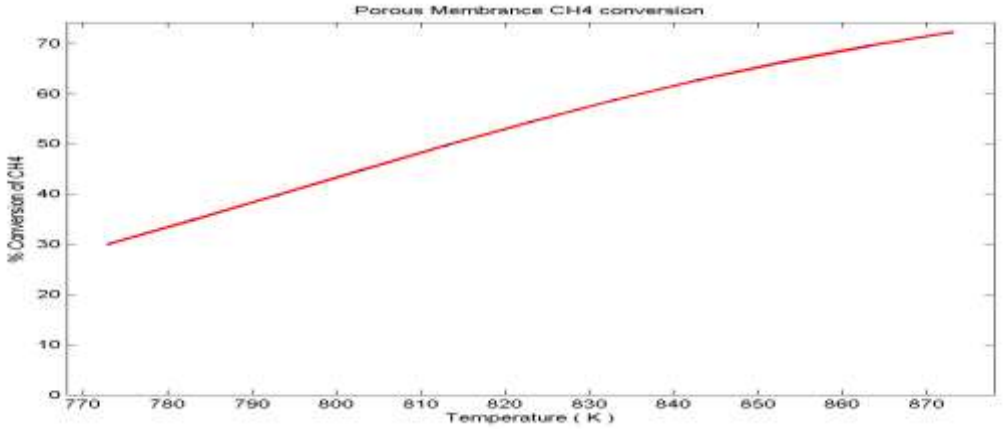

Fig.17: Effect of temperature on methane conversion in porous membrane reactor.

 DOI : 10.35291/2454-9150.2020.0609

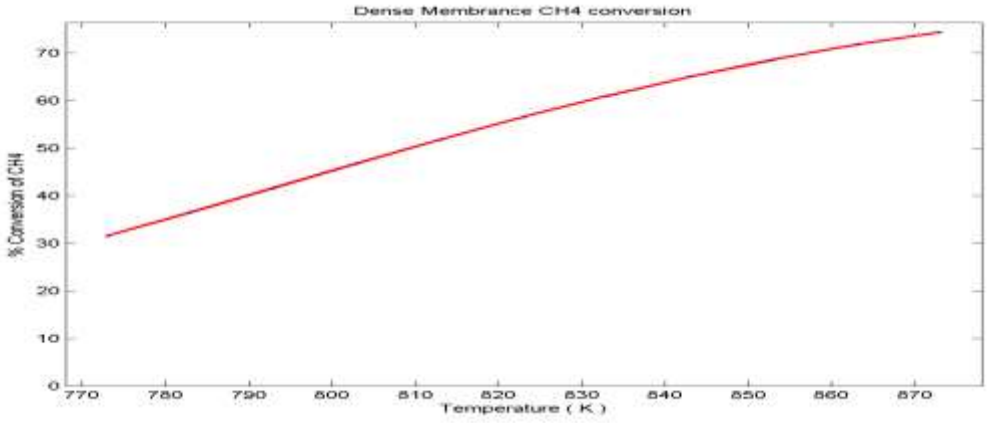

Fig. 18: Effect of temperature on methane conversion in dense membrane Reactor.

Effect of temperature on CO_2 conversion in porous MR & dense MR

The graphs show that the conversion of CO_2 is found to be more than CH_4 conversion. As we know that the CH_4 & CO_2 are involved in several secondary reactions which occur during the methane dry reforming. Moreover due to the endothermicity of the reaction system, CO_2 conversion increases with increasing temperature like the CH_4 conversion. This phenomenon can be illustrated as in the MRs the reverse reaction is favoured by the selective permeation of CO with respect to CO_2 throughout the porous Pd-Ag membrane.

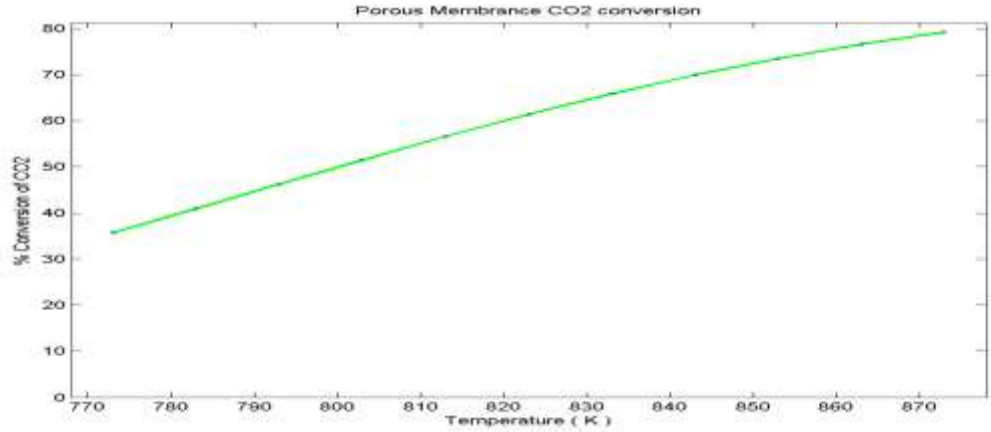

Fig. 19: Effect of temperature on CO_2 conversion in porous membrane reactor.

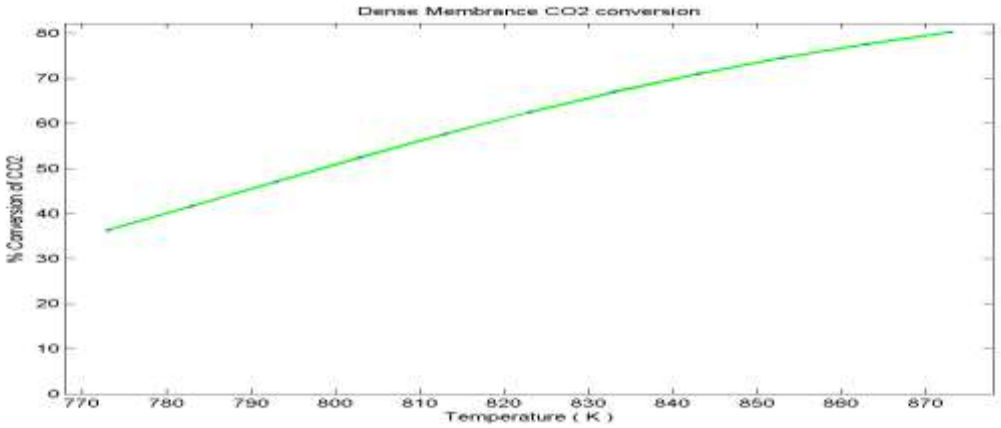

Fig. 20: Effect of temperature on CO_2 conversion in dense membrane reactor.

Effect of temperature on selectivity of H_2 in porous MR & dense MR.

As far as the selectivity is concerned, from the figures it is evident that there is no pronounced effect of temperature on selectivity of H_2 for both the porous MR and dense MR. The selectivity of H_2 for porous and dense MR varies at around 15.9 & 2.4 respectively.

 DOI : 10.35291/2454-9150.2020.0609

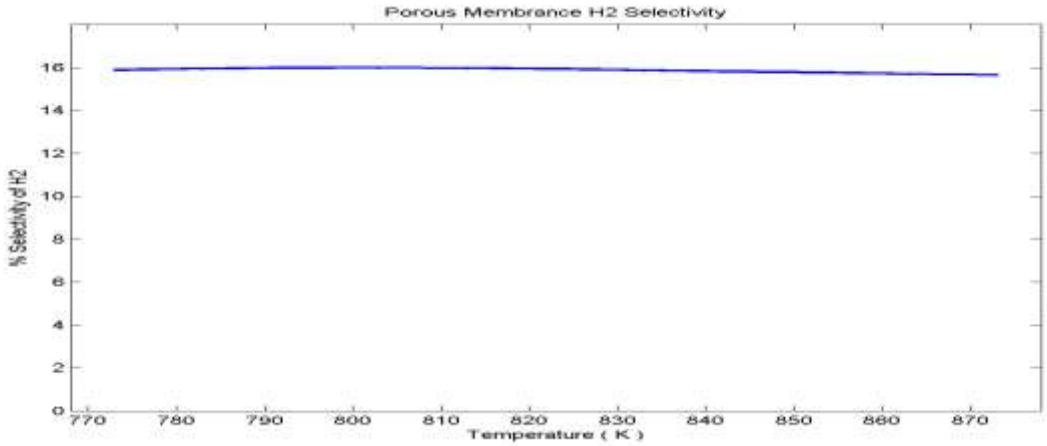

Fig. 21: Effect of temperature on selectivity of H_2 porous membrane reactor.

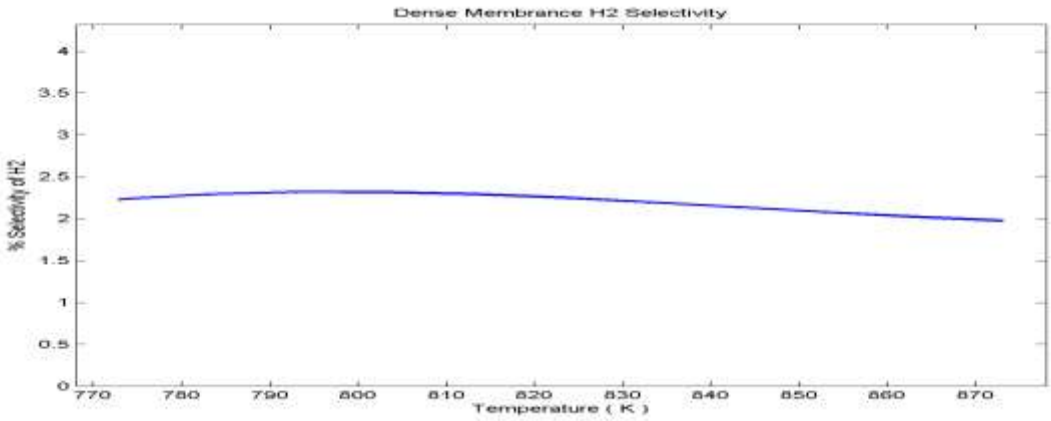

Fig.22: Effect of temperature on selectivity of H_2 in dense membrane reactor.

Effect of temperature on selectivity of CO in porous MR & dense MR.

From the figures 23 & 24 it is observed that the selectivity of CO is higher than H_2 selectivity for both the MRs. Since H_2 and CO are produced by the reaction 1 but part of this hydrogen reacts with CO_2 by reactions 2 & 3 producing both other CO and CH_4 and consuming CO_2 for this reason the CO selectivity is higher than H_2 selectivity.

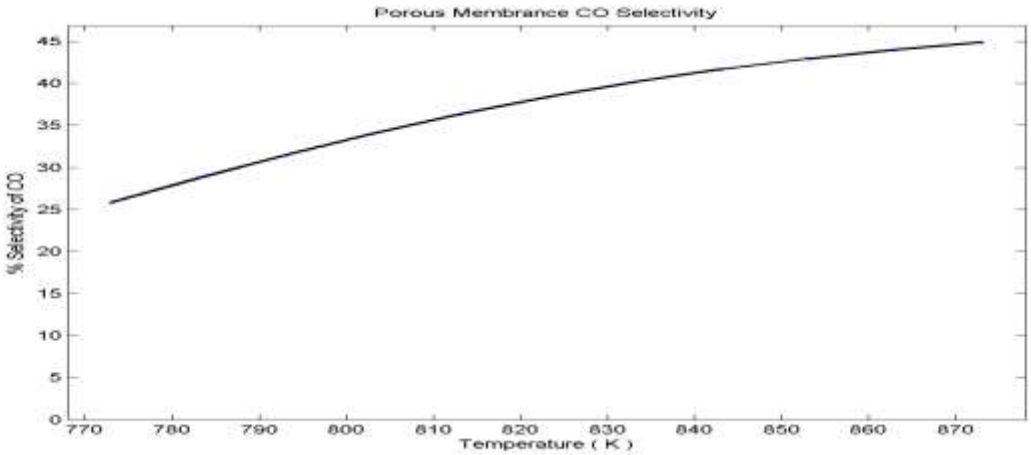

Fig. 23: Effect of temperature on selectivity of CO porous membrane reactor.

 DOI : 10.35291/2454-9150.2020.0609

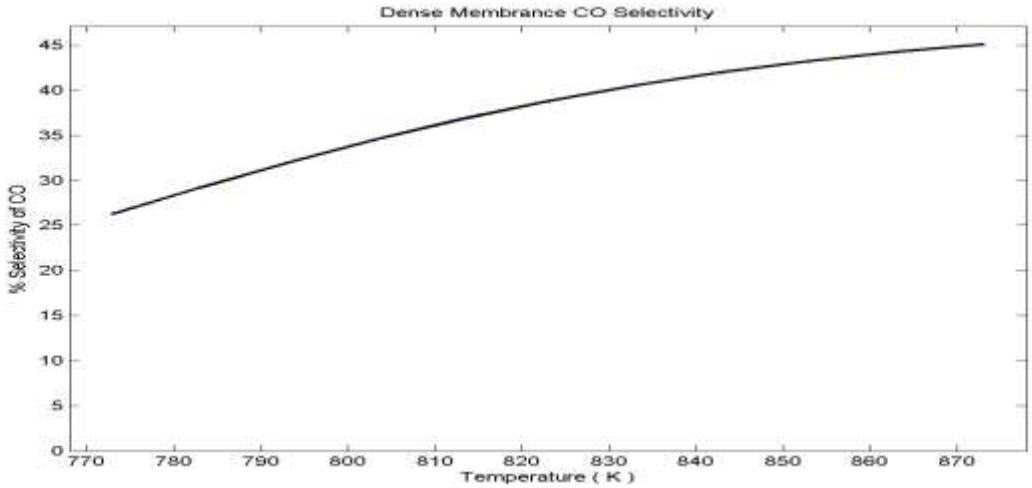

Fig. 24: Effect of temperature on selectivity of CO dense membrane reactor.

VII. CONCLUSION

In this work a one dimensional isothermal mathematical model is taken to analyze the performance of porous membrane reactor (MR), dense membrane reactor (MR) and FBR of using same Pd-Ag Membrane. The catalyst used in all different reactors is Ni-Al_2O_3. Here the performance of porous and dense MR is compared with the FBR. The simulation results show that the conversion of CH_4 is higher in FBR than Porous MR but it is lesser than the dense MR at all temperature range. It is due to the continuous removal of products from the reaction side of the reactor also the conversion in FBR is limited by temperature. The conversion in FBR increases with the increase in temperature but after 873K it does not increases for that purpose MRs porous and dense have been used. The yield of CO is higher than the yield of H_2, for all the reactors, which increases with increase in temperature whereas the CO_2 conversion is more in porous MR than the FBR.

When performed in the porous Pd–Ag membrane reactor the dry methane reforming is a useful reaction system for the carbon dioxide consumption. In fact, the maximum CO_2 conversion is 20.6% for the MR at 723K, versus the corresponding value of 14% achieved with the FBR. While, the maximum CH_4 conversion is 17.41% for the FBR at 723K, versus the corresponding value of 8.4% achieved with the MR. On the other hand, by using the dense Pd–Ag membrane reactor the reaction system is a useful way for hydrogen production being the hydrogen recovery higher than 25% at 723K. So, in this case, the choice of the reactor type could depend on the goal of the reaction system. Moreover, at higher reaction temperature (673 and 723K) the MRs gives lower deposition of carbon with respect to the FBR. In particular the lower carbon deposition is obtained when the dense membrane is used. Resuming the advantages of the MR with respect to a FBR it can be said that, in case of porous membrane the CO_2 conversion is close to the equilibrium value and the carbon deposition is lower than the one observed in the FBR; while in the case of dense membrane, the CH_4 conversion is close to the equilibrium value and the carbon deposition is lower than the one observed in the FBR. Moreover, increasing the pressure corresponds to an increase of the methane conversion which is higher than the corresponding thermodynamic equilibrium value for a FBR operating in the same experimental conditions. Last but not least, in the case of dense membrane a CO-free hydrogen stream is obtained in shell side of the reactor while in any case a FBR is always producing a stream containing both CO and H_2. Generally, these considerations make the membrane reactor a very interesting device for the methane dry reforming reaction.

VIII. RECOMMENDATION

Hydrogen is emerging as a future replacement fuel for the traditional fossil fuels that will be capable of satisfying our future energy demands. Hydrogen energy systems can emerge to be cleaner, more reliable, and much more efficient; thus possibly ensuring our energy security and environmental viability. One of the many major challenges of a future hydrogen energy economy is the reduction in the cost of production, storage of hydrogen. Pure hydrogen can be obtained through the dense MR with the temperature investigated, an increase in temp yields more H_2 production.

However, the hydrogen gas permeating through the dense membrane increases the carbon deposition in the Boudouard reaction which occurs as side reaction. Due to this important key factor a deeper work is needed to better understand the effect of the dense membrane on the carbon deposition.

The different reactors were used to see the conversion and selectivity in all reactors, so different membranes should be manufactured for the selective permeation of the components which shift the equilibrium to the desired direction for the maximization of the hydrogen production.

 DOI : 10.35291/2454-9150.2020.0609

The method adopted for the different reactors are solved, a cost analysis can be made for this work.

NOMENCLATURE

d	Thickness of the membrane, [m]
d_p	Membrane pore diameter [m]
D_i	Effective permeability of i^{th} component [mol/m^2-atm-s]
E_a	Apparent activation energy [kJ/mol]
F_i	Molar flow rate of i^{th} component in shell/tube side of reactor [mol/s]
$F_{i,0}$	Initial molar flow rate of i^{th} component in the shell side [mol/s]
$F_{i,1}$	Exit molar flow rate of i^{th} component in the shell side [mol/s]
$F_i^{'}$	Initial molar flow rate of i^{th} component in tube side [mol/s]
$F_{i,0}^{'}$	Exit molar flow rate of i^{th} component in tube side [mol/s]
J_H	Hydrogen flux through the dense membrane [mol/m^2-s]
J_1	Molar flux of i^{th} component through membrane [mol/m^2-s]
k_1	Rate constant for dry reforming reaction [mol/ (g-bar-hr)]
k_2	Rate constant for RWGS reaction [mol/(g-bar-hr)]
K_{CH_4}	Adsorption equilibrium constant of methane [atm-1]
L	Reactor length [m]
M_i	Molecular weight of i^{th} component [g/mol]
Δp	Trans-membrane pressure difference [Pa]
p_{lumen}	Pressure in the lumen side [Pa]
p_{shell}	Pressure in the shell side [Pa]
$P_{H_2}^{lumen}$	Hydrogen partial pressure in the lumen side [Pa]
$P_{H_2}^{shell}$	Hydrogen partial pressure in the shell side [Pa]
$P_{H_2}^{o}$	Pre-exponential factor [mol/(m^{2}skPa$^{0.5}$)]
P_t	Total pressure on tube side [atm]
R	Universal gas constant [J/mol-K]
r_1	Forward rate of dry reforming reaction [mol/m^3-s]
r_2	Forward rate of RWGS reaction [mol/m^3-s]
R_1	Inner radius of the tube[m]
R_2	Outer radius of the tube[m]
T	Absolute temperature [K]

REFERENCES

[1] Becerra A.M., Maria E. Iriarte, & Adolfo E. Castro-Luna (2003) "Catalytic activity of a nickel on alumina catalyst in the CO_2 reforming of methane", React. kinet. catal. lett. vol. 79, No 1, 119-125.

[2] Coronas J., & J. Santamaría, (1999)."Catalytic reactors based on porous ceramic membranes". Catalysis Today. 51 (3-4). 377-389.

[3] Dittmeyer R., Volker Hollein, & Kristian Daub (2001) "Membrane reactors for hydrogenation and dehydrogenation processes based on supported palladium", J. of molecular catalysis A: Chemical 173, 135-184.

[4] Dixon A.G. (2003) "Recent research in catalytic inorganic membrane reactors", International J. of chemical reactor engineering Volume 1, Review R6.

[5] Froment G. F. (2000). "Production of Synthesis Gas by Steam- and CO_2-reforming of Natural Gas". Journal of Molecular Catalysis A: Chemical. 163(1-2): 147-156.

[6] Gallucci, F., L. Paturzo, & A. Basile, (2004) "A simulation study of steam reforming of methane in a dense tubular membrane reactor". International Journal of Hydrogen Energy. 29(6): 611-617.

 DOI : 10.35291/2454-9150.2020.0609

[7] Gallucci F., S.Tosti, & A. Basile (2008) "Pd-Ag tubular membrane reactors for methane dry reforming: a reactive method for CO_2 consumption and H_2 production", J. of membrane science 317, 96-105.
[8] Galuszka, J., R. N. Pandey, & S. Ahmed, (1998). "Methane conversion to syngas in a palladium membrane reactor". Catalysis Today. 46(2-3): 83-89.
[9] Garcia-Garcia F.R., M.A. Soria, C. Mateos-Padrero, A. Guerrero-Ruiz, I. Rodriguez-Ramos, & K. Li (2013) " Dry reforming of methane using Pd-based membrane reactors fabricated from diffirent substartes". Journal of Membrane Science 435, 218-225.
[10] Kumar Shashi, Sukrit Shankar, Pushan R. Shah, & Surendra Kumar (2006) "A comprehensive model for catalytic membrane reactor", International Journal of Chemical Reactor Engineering, Vol. 1, 234-256.
[11] Kumar S., Mohit Agrawal, Surendra Kumar, & Sheeba Jilani (2008) "The production of syngas by dry reforming in membrane reactor using alumina-supported Rh catalyst: a simulation study" International J. of Chemical Reactor Engineering Vol6 Article A109.
[12] Nielsen J.R.R. (1993) "CO_2 reforming of methane over transition metals", J.Catal., Vol 144, 38-49.
[13] Nielsen J.R.R. (2002) "Syngas in prespective", Catalysis today 71, 243-247.
[14] Olsbye U., Thomas Wurzel, & Leslaw Mleckzo (1997). "Kinetic and reaction engineering studies of dry reforming of methane over Ni/ La/Al_2O_3 catalyst" Ind. Eng. Chem.36, 5180-5188.
[15] Prabhu A.K, A. Liu, L.G. Lovell, & S.T. Oyama (2000) "Modeling of the methane reforming reaction in hydrogen selective membrane reactors", J. of membrane science 177, 83-95.
[16] Sirkar K.K., Purushottam V. Shanbhag, & A. Sarma Kovvali (1999) "Membrane in a reactor: A functional perspective", Ind. Eng. Chem. Res 38, 3715-3737.
[17] Van Ness, H.C., Smith, J.M., and Abott., M.M., (2004)"Introduction to Chemical engineering Thermodynamics", Mc Graw Hill Sci.Eng.,USA, Ed^n 7

 DOI : 10.35291/2454-9150.2020.0609